A combined wear-fatigue design methodology for fretting in the pressure armour layer of flexible marine risers

A combined wear-fatigue design methodology for fretting in the pressure armour layer of flexible marine risers

S.M. O'Halloran[1], P.H. Shipway[2], A.D. Connaire[3], S.B. Leen[1*], A.M. Harte[4*]

[1] Mechanical Engineering, National University of Ireland, Galway, Ireland

[2] Faculty of Engineering, University of Nottingham, Nottingham, UK

[3] Wood Group Kenny, Galway Technology Park, Parkmore, Galway, Ireland

[4] Civil Engineering, National University of Ireland, Galway, Ireland

* Joint senior researchers on this project

Abstract

This paper presents a combined experimental and computational methodology for fretting wear-fatigue prediction of pressure armour wire in flexible marine risers. Fretting wear, friction and fatigue parameters of pressure armour material have been characterised experimentally. A combined fretting wear-fatigue finite element model has been developed using adaptive meshing technique and the effect of bending-induced tangential slip has been characterised. It has been shown that a surface damage parameter combined with a multiaxial fatigue parameter can accurately predict the beneficial effect of fretting wear on fatigue predictions. This can provide a computationally efficient design tool for fretting in the pressure armour layer of flexible marine risers.

1 Introduction

Fretting is a form of surface damage that occurs between nominally static surfaces in contact experiencing cyclic tangential loading resulting in a non-uniform, small-scale

(typically micro- or nano-scale) relative slip between both surfaces. Dobromirski [1] proposed that there are up to 50 variables that affect fretting behaviour. There are three slip regimes associated with fretting [2], (i) partial slip (PS), (ii) gross slip (GS), and, (iii) mixed slip (MS). The slip regime is dependent on loading conditions (normal and tangential loads) and the coefficient of friction (COF) between the two surfaces [1]. Vingsbo and Söderberg observed the relationship between applied slip amplitude, fatigue life and wear rate for a fretting fatigue test (Figure 1). There is little effect of wear in the stick region and since there is little or no relative motion, high fatigue life is observed. Partial slip occurs as slip amplitude increases; wear remains low in this slip regime, but fatigue life decreases dramatically reaching a minimum value at the partial-gross slip transition. In gross slip, wear becomes the predominant damage mechanism and fatigue life increases; this has been attributed [3] to embryonic cracks being “worn away” before they nucleate to a significant length. Leen and co-workers [4] have also shown that this increase can be attributed and, in particular, predicted on the basis of the wear-induced re-distribution of contact stresses. In addition to contact load and slip amplitude, COF and wear coefficient are key variables in this tribological process.

Fretting is a potential problem in many engineering applications such as spline couplings, eg. aero-engine main shaft splines [5 - 6], gas turbine dovetail joints [7], steel wire ropes [8 - 9], flexible marine risers [10 - 11] and other industrial applications. Flexible marine risers are a key component in the delivery of offshore hydrocarbons from the seabed to sea level, typically to a floating structure, such as a platform or vessel. In recent decades, flexible marine risers have transformed the oil and gas industry, allowing for hydrocarbon extraction at deeper depths and higher pressures in comparison to the traditional rigid structures. The structural integrity of flexible risers is paramount to personnel and environmental safety. Also, the economic implications of riser failure are significant. Flexible risers rely on a

complex, composite cross-sectional architecture of helically-wound, interlocking steel wires and polymer layers to give a unique combination of high bending flexibility, axial and torsional stiffness and internal pressure resistance, as well as internal and external corrosion resistance (see Figure 2) [12]. The research presented here focuses on the helically-wound, interlocked metallic wires which form the pressure armour layer; the primary function of this layer is to contain internal pressure and resist hoop stress. For the inter-locking steel wires, micro-articulation of the nub and groove mechanical contacts (Figure 2) plays a key role in achieving the complex combination of exceptional mechanical properties. In flexible risers, normal forces due to internal hydrocarbon and external hydrocarbon pressure as well as radial stresses from the tensile armour layer keep the nub and groove of the pressure armour in contact. Failure of these sub-layers due to fatigue is one of the main concerns during the service lifetime of the flexible riser.

The effects of fretting wear and fretting fatigue on flexible risers is difficult to analyse and solve and so it is not presently considered during design of flexible risers. The American Petroleum Industry (API) design codes recommend a safety factor of 10 for fatigue design of pressure armour layers [13], to account for uncertainties, including fretting, for example.

In marine risers, fretting action may be caused by cyclic loads such as shearing loads due to bending or fluctuations in hydrocarbon pressure. Hence, there is a potential for micro-scale cyclic frictional contact stresses and slip leading to micro-scale surface damage, typically, a combination of wear and fatigue micro-crack nucleation, ultimately leading to loss of function and fatigue cracking and failure. The predominance of wear or fatigue crack nucleation is dependent on a large number of mechanical and physical variables; therefore the development of a combined modelling and experimental capability is critical for a service life prediction (design) methodology, fretting behaviour in the pressure armour layer of flexible marine risers has been identified as an aspect of riser design which requires further research

[14]. Løtveit and Bjaerum [15] identified fretting of the pressure armour wire as a potential failure mode for flexible marine risers. The problem of fretting fatigue in flexible marine risers has received relatively little attention. Féret [16] presented a theoretical approach to calculate stresses, contact pressures and slip between tensile armour layers of flexible pipes under axisymmetric loading. Burke and Witz [10] presented an excellent review of the problem at an industrial conference. More recently, Perera [17] presented an experimental investigation for fretting of the pressure armour layer of unbonded flexible pipes.

In this paper, experimental testing on representative pressure armour steel is presented for identification of friction and wear parameters. Fatigue testing of the pressure armour wire material is presented. Multiaxial fatigue methodology is implemented along with adaptive meshing technique for wear simulation. Explicit wear-fatigue modelling is used to characterise the effect of bending induced tangential slip on fatigue life. Furthermore, it is shown that a fretting surface damage parameter combined with the multiaxial fatigue parameter can successfully predict the beneficial effect of wear-induced stress re-distribution on fatigue. This approach has significant advantages for flexible riser fretting fatigue design.

2 Computational methodology

2.1 Finite element model

Previous work by the authors has focused on fretting contact in the nub-groove contact area using an axisymmetric flexible riser model [11]. In this work, a generalised round-on-flat geometry has been used to reduce the computational time of the models. It has been shown that a round-on-flat is more critical in terms of fretting fatigue life in comparison to a flat on flat geometry [18]; thus, a generalised round-on-flat 2D nub-groove geometry has been simulated.

A two-dimensional, plane strain assumption has been adopted for each case. The material used is a carbon steel, with a Young's modulus of 189 GPa and a Poisson's ratio of 0.3. The radius of the cylinder is 3 mm. A COF of 0.75 was used, based on fretting fatigue tests on representative pressure armour layer material.

Since the analysis is a frictional contact problem, two-dimensional, 4-noded, quadrilateral, plane strain elements were used due to their accuracy and stability for these loading conditions [19]. A mesh sensitivity study was used to establish a converged mesh; the resulting mesh is highly refined in the contact region, becoming coarser further from the contact area (see Figure 3). The contact element size is approximately 10 μm × 10 μm. The transition between fine mesh and coarse mesh is achieved by reducing the mesh density through an unstructured mesh between the fine and coarse meshes.

The master-slave algorithm for finite sliding contact within Abaqus was used to define the surface interaction for both models. The maximum allowable penetration depth between master and slave nodes was set to 1 μm. The adjustment tolerance for the initial geometry was set to 0.001 μm. Since Coulomb-Amontons' Law is assumed for sliding friction, the exact stick condition is ensured by implementing Coulomb friction based on the Lagrange multiplier contact algorithm.

The dimensions of the substrate material were made significantly larger than the contact area so that the assumption of an elastic half-space remained valid. The bottom edge of the substrate was restrained in the z direction and the left and right edges were restrained in the x direction.

The normal load per unit length, P = 50 N/mm, is applied to the cylinder, and a superimposed cyclic tangential displacement (Δ) is applied as shown in the loading history of Figure 4.

2.2 Fatigue model

For fretting fatigue cracks, the stress range is a primary parameter for the calculation of fatigue life. High shear stress (τ_{xz}) ranges are generally considered to be responsible for fatigue crack initiation, and high tangential (trailing edge) stress (σ_{xx}) ranges for Mode I fatigue crack propagation. Since the contact loading is cyclic, a material point can experience a high shear stress and a low tangential stress at one instant in a cycle, and subsequently at a later instant (e.g. half-cycle later) a low shear stress and a high tangential stress; this behaviour increases the possibility of crack formation and growth due to fretting. Fretting fatigue crack initiation and growth can occur under both low and high cycle fatigue conditions, depending inter-alia on local stresses, material strength and frictional and wear conditions.

The Smith-Watson-Topper (SWT) fatigue parameter [20] combines both the Coffin-Manson equation for low cycle fatigue (LCF) and Basquin's equation for high cycle fatigue (HCF), as follows:

$$SWT = \frac{\sigma_{\max}\Delta\varepsilon_a}{2} = \frac{(\sigma'_f)^2}{E}(2N_i)^{2b} + \sigma'_f\,\varepsilon'_f\,(2N_i)^{b+c} \tag{1}$$

where σ_{max} is the maximum normal stress on the critical plane (for mean stress effect), $\Delta\varepsilon_a$ is the maximum normal strain amplitude on the same plane, E is Young's modulus, σ'_f and b are fatigue strength coefficient and exponent, ε'_f and c are the fatigue ductility coefficient and exponent, and N_i is the number of cycles to crack initiation.

It has been observed that fatigue cracks initiate and grow on preferential planes within a material, where the orientation depends on the normal stresses and strains on the plane. A

2D critical-plane implementation of the SWT parameter has previously been validated for fretting fatigue by the authors [11] based on the previous work of Leen and co-workers [4, 21] is incorporated. This is a combined stress and strain transformation (covering 360° in 5° increments) process, applied to the FE models of the pressure armour layer, to identify the critical plane value and orientation from the history of cyclic multiaxial stresses and strains on each candidate plane. Equation ((1) is then solved numerically using a Newton-Raphson solution scheme to predict the number of fretting cycles to crack nucleation. Sum et al. [21] showed that the critical plane approach can capture stress gradient effects, such as contact size [22, 23], similar to the volume averaging method used by other researchers [24]. This was attributed to the inherent averaging nature of the Gauss sampling technique in the FE method.

2.3 Wear model

The wear model utilised here is an adaptive mesh methodology in Abaqus using an implementation of UMESHMOTION user sub-routine to simulate the fretting wear process and is based on the modified Archard wear equation proposed by McColl et al. [19]. The fretting wear depth is calculated by applying Archard's equation to the local contact conditions along the contact area. The local wear depth is given by [21]:

$$\Delta h(x,t) = k_l\, p(x,t) s(x,t) \tag{2}$$

where $\Delta h(x, t)$, $p(x, t)$ and $s(x, t)$ are the incremental wear depth, contact pressure and relative slip at a point x on the contact surface at time t and k_l is the local wear coefficient. McColl et al. [19] describes how the FE simulation of wear requires a local wear coefficient, k_l, which is expressed as the wear per unit local slip per unit local contact pressure. However

this is wear coefficient, k, per unit displacement per unit load (as described later in Section 3.1). It has been shown [19, 23] that there is a close relationship between the local wear coefficient k_l and the experimentally found volumetric wear coefficient k.

To reduce the computational time for fretting wear simulations, a cycle jumping technique [19, 24] was employed, where it is assumed that the contact pressure and slip distributions remain constant over ΔN cycles. Therefore Equation ((2) becomes:

$$\Delta h(x,t) = \Delta N k_l \, p(x,t) s(x,t) \tag{3}$$

The implementation of this wear simulation algorithm in Abaqus is represented in the flowchart of Figure 5 and the adaptive meshing technique is depicted in Figure 6.

The cycle jump used in this study is ΔN = 1,000 with 100 increments in on tangential fretting cycle.

2.4 Combined wear-fatigue model

Due to the evolving geometry and stress fields associated with fretting wear, a fatigue damage accumulation model is required for prediction of fretting fatigue life. The Miner-Palmgren rule is used to calculate the damage accumulation, as follows:

$$D = \sum_{i=1}^{N} \frac{\Delta n}{N_i} \tag{4}$$

where Δn is the number of cycles experienced at loading cycle i with an associated SWT value of SWT_i, and N_i is the predicted number of cycles to crack initiation for SWT_i (given by Equation ((1). When D = 1, a crack is assumed to have initiated at the SWT-predicted

location, orientation and number of cycles. Within the present FE methodology, *D* is calculated at the centroid of each surface element.

As discussed in detail by Zhang et al. [27], the effect of wear via the adaptive meshing technique in the FE simulation is that the centroidal position of each surface element changes from cycle to cycle, due to material removal and therefore damage cannot be accumulated at the same centroidal position from cycle to cycle (see Figure 6). Hence following Zhang et al. [27], a material point mesh (MPM) has been defined, independent of the FE mesh, to calculate the damage accumulation. In this method the MPM has fixed coordinates; the SWT damage is calculated at the centroid of each element and linearly interpolated back to the MPM for calculation of accumulated damage.

3 Experimental

3.1 Fretting wear tests

Due to the size and complexity of geometry of the formed (extruded) pressure armour wire (see Figure 7) it is difficult to extract fretting wear test specimens for laboratory scale fretting tests (eg. See Figure 8) from the wire itself. Hence, in this work an EN8 metal with similar chemical composition as that of pressure armour wire material (see Table 1) has been selected for fretting wear tests.

Cylinder-on-flat fretting wear tests were carried out at the University of Nottingham under loading conditions as shown in Table 2. The cylinder radius, *R*, was 6 mm and specimen width, *W*, was 10 mm (see Figure 8). Tests were conducted for 10^5 fretting cycles at a frequency of 20 Hz. From these tests, the coefficient of friction (COF) evolution with fretting cycles is presented in Figure 9. The COF starts off at about ~0.2 and increases rapidly to ~0.6, due to material transfer and adhesion during metal on metal contact; an additional

increase is then observed due to the abrasive action during the accumulation of oxidised debris; the COF eventually stabilises (typically) to a constant value (~0.7-0.8) as the abrasive action decreases due to the formation of compacted debris. Increased fretting damage was observed with increasing applied displacement and normal load.

Since there is no way to measure the local contact slips and local contact pressure, the wear coefficient has been calculated using applied loading conditions (normal load, P^* and applied slip, S). In this work a three-dimensional wear volume, V, was measured using a Bruker Contour GT-I interferometer. This provided data to calculate the Archard wear coefficient using the equation:

$$\frac{V}{S} = kP^* \tag{5}$$

where V is the wear volume, S is the applied displacement, k is Archard wear coefficient and P^* is the normal load applied to the specimen. An average wear coefficient was calculated as 1×10^{-8} MPa^{-1}. This methodology of calculating the wear coefficient is more accurate that that previously used by McColl et al. [19] where and averaged wear coefficient was calculated using average wear scar depths measured using two dimensional profilometry. Following McColl et al. [19] it is assumed here that the wear rate is independent of contact geometry, i.e. the Archard wear coefficient is assumed to be applicable to contact geometries other than that tested.

3.2 Tensile and fatigue tests

Monotonic tensile tests have been conducted on the pressure armour material extracted from a pre-service flexible marine riser using the NUI Galway Instron servo-

hydraulic testing machine and a video extensometer. The stress-strain curve of this test is presented in Figure 10, these tests have measured an ultimate tensile strength of σ_{UTS} = 900 MPa and a Young's modulus of 189 GPa.

A program of low cycle fatigue (LCF) tests has been conducted on pressure armour material extracted from a pre-service flexible marine riser. A modified fatigue specimen geometry, based on the ASTM E606-04 [28] standard for strain-controlled fatigue testing has been designed to facilitate extraction from the pressure armour wire itself, following straightening. Strain-controlled cyclic tests were carried out using the Instron servo-hydraulic testing machine, with servo-hydraulic grips and a contact extensometer for strain feedback. Tests were conducted at strain ranges of 0.8%, 1%, 1.25% and 2%. These tests have provided Coffin-Manson constants (ε'_f and c) for the computational fatigue model (see Table 3).

Pending high cycle fatigue (HCF) tests, the universal slopes method [25 - 26] has been used to estimate the Basquin constants (σ'_f and b) for the computational fatigue model (see Table 3). This method gives estimated fatigue coefficients based on monotonic tensile test results for ultimate tensile strength, σ_{UTS}, e.g. $\sigma'_f = 1.9\sigma_{UTS}$, and b = -0.12.

4 Results and discussion

4.1 Model validation

The SWT fatigue model used was previously [11] validated against experimental results [3] for the partial slip regime.

The fretting wear model implemented has also been validated against experimental wear scar profiles. Figure 11 presents a comparison between finite element simulated wear scars and experimentally measured fretting wear scars for R = 6 mm under two different

loading conditions: (a) P^* = 500 N, Δ^* = 30 μm; and (b) P^* = 250 N, Δ^* = 15 μm. These loading conditions give a range of contact pressures and relative slips that are representative of those in nub-groove contact in pressure armour layer. There is a good correlation between the FE simulated wear scar and the experimentally measured wear scar.

In this study, as a simplification, wear of the indenter and the effect of debris is not explicitly simulated.

4.2 Effect of wear on stresses

Figure 12a presents the evolution of wear with fretting cycles for 3 mm cylinder-on-flat model under P = 50 N/mm and Δ = 10 μm; These loading conditions give gross slip conditions, and therefore, wear is the dominant fretting damage. Figure 12b presents the corresponding contact pressure for the 1st, 25,000th, 100,000th and 200,000th cycles. It can be seen that as wear evolves, the contact width widens and the contact pressure is redistributed over a wider area; therefore the peak pressure is dramatically reduced and the pressure is much less concentrated than for the initial fretting loading.

The effect of the redistribution of contact pressure on (a) tensile (σ_{xx}) and (b) shear (τ_{xy}) stresses is presented in Figure 13. The contact width is increased from 100 to 360 μm over 2×10^5 fretting cycles. This causes a 55 % decrease in trailing edge tensile stress value. The location of the maximum (trailing edge) tensile stress moves outwards as the contact width increases. The maximum shear stress value is initially located in the centre of contact; however, as the contact width increases, the shear stress is redistributed to an almost uniform value across the contact, which is dramatically reduced relative to the unworn case (about 75 % less that the initial peak value).

4.3 Crack Initiation

Fretting crack initiation life predictions have been calculated based on the number of cycles to crack initiation at a depth of 5 μm into the substrate. This work focuses on the interaction and competition between fatigue crack initiation (damage) and wear-induced material removal, potentially leading to either exacerbated initiation conditions (partial slip) or ameliorated conditions (gross slip). Crack propagation is not considered in this work. Future work may focus on this aspect

Figure 14 presents the predicted effect of applied displacement on crack initiation life with and without the effects of wear-induced material removal. In the partial and mixed slip regimes (Δ < 4 μm), the predicted crack initiation life is essentially the same for both models. However, in the gross slip regime, excluding of wear effects is seen to significantly under predict life. Including wear effects leads to a dramatic increase in life (to over 10^8 cycles) with increasing stroke/displacement relative to the minimum value of the partial slip-gross slip transition. In all cases, the fretting fatigue cracks are predicted to initiate at the edge of contact. The predicted critical plane angle for crack initiation is between 10° and 30° to the x-axis (as shown in Figure 6).

The predicted increase in fretting crack initiation life when fretting wear is included is attributed to the redistribution of stresses, due to the widening of the contact width and evolution of the contact geometry. This trend is consistent with the fretting schematic of Vingsbo and Söderberg [2] (Figure 1), where, as wear rate increases, the predicted fretting fatigue life increases. Hence, for flexible marine riser design, fretting wear needs to be considered in gross slip fretting analysis of the nub-groove contact, to avoid overly conservative prediction of fretting crack initiation.

4.4 Simplified life prediction including the effect of wear

Adaptive mesh techniques are too computationally expensive. The computational time for simulating fretting wear in a full or partial flexible marine riser, with multiple three-dimensional nub-groove contacts under realistic loading histories is prohibitiroly expensive for design purposes. Hence, it is proposed to adopt the D_{fret} fretting design parameter as proposed by Ding et al. [31], The D_{fret} method introduces a surface damage factor for the effects of fretting wear to a modified SWT approach, developed to incorporate the effects of slip and surface wear damage on crack initiation, as follows:

$$\sigma_{\max}\Delta\varepsilon_a D_{fret} = \frac{(\sigma'_f)^2}{E}(2N_i)^{2b} + \sigma'_f\,\varepsilon'_f\,(2N_i)^{b+c} \tag{6}$$

where D_{fret} is a surface damage factor given by [31]:

$$D_{fret} = (1 - C\tau\delta)\left\langle 1 - \frac{\tau\delta}{(\tau\delta)_{th}}\right\rangle^m \tag{7}$$

where C, m, and $(\tau\delta)_{th}$ are material constants.

$(\tau\delta)_{\text{th}}$ has been estimated here as a value slightly greater than the value at the partial slip - gross slip transition, based on FE simulations. For $\tau\delta < (\tau\delta)_{\text{th}}$ the unmodified SWT value is used (i.e. $D_{\text{fret}} = 1$); for $\tau\delta > (\tau\delta)_{\text{th}}$ the SWT-D_{fret} value is used (Equation (7)).

The material constants C and m were found by applying a least squares minimisation method to the following objective function:

$$F(C,m) = \sum_i \left\{SWT_{D,i}(C,m) - SWT_{AM,i}\right\}^2 \tag{(8)}$$

where $SWT_{D,i}(C,m)$ is the D_{fret} predicted SWT value at sample (element centroid) point *i*, $SWT_{AM,i}$ is the corresponding wear-simulated SWT value (using adaptive meshing technique). The material constants found for the pressure armour layer are presented in Table 4. A comparison of wear simulated $SWT_{\max}$ and the corresponding maximum *SWT*-D_{fret} value, (from the least squares minimisation method) is shown in Figure 15.

A comparison between the fretting crack initiation lives calculated using wear simulation analysis and the modified SWT-D_{fret} parameter is presented in Figure 16. This shows excellent correlation between the two prediction methods, particularly in terms of the beneficial effect of increasing (gross) slip amplitude. The major advantage of the modified SWT parameter over explicit modelling of wear is the significant reduction in computational expense. Future work will experimentally verify the $(\tau\delta)_{\text{th}}$ constant for pressure armour layer material.

5 Conclusion

- Tensile and fatigue tests of pressure armour layer material has been conducted for characterisation of material properties. Fretting wear tests have been carried out under representative loading conditions on a representative pressure armour material with essentially the same chemical composition and hardness as pressure armour layer material. These tests have characterised the tribological behaviour of the nub-groove contact in the pressure armour layer.
- A finite element model of a cylinder-on-flat geometry that is representative of nub-groove frictional contact has been developed. This computational methodology combines fretting wear simulation using adaptive meshing techniques and critical

plane multiaxial fatigue life predictions. The fretting wear finite element simulations have been validated against cylinder-on-flat fretting wear experimental test results.

- The effect of tangential displacement on fretting crack initiation life has been investigated. In partial slip, wear rate is low and therefore a detrimental effect on number of cycles to crack initiation is observed. However, in gross slip wear has a beneficial effect on predicted fretting crack initiation life due to the re-distribution on stresses association with material removal caused by wear.
- A combined surface damage and multiaxial fatigue parameter has been shown to successfully predict the effect of wear and tangential displacement on predicted fretting crack initiation life. The major benefit of this parameter is the reduced computational expense since wear does not have to be explicitly modelled. This is a key development in terms of the design of flexible risers against fretting.

Acknowledgements

The authors would like to thank the Irish Research Council and Wood Group Kenny for funding of this project through the Enterprise Partnership Scheme, National University of Ireland for funding through an NUI Travelling Scholarship. We also wish to acknowledge the help and support we have received from Mr. Kieran Kavanagh (Wood Group Kenny), the NUI Galway Engineering Building technical staff; particularly Mr. Bonaventure Kennedy and Mr. Patrick Kelly and the Facility of Engineering at the University of Nottingham.

References

[1] J. M. Dobromirski, “Variables in the Fretting Process: are There 50 of Them? Standardisation of Fretting Fatigue Test Methods and Equipment,” *ASTM:* M.H. Attia (Eds.), R.B. Waterhouse, 1992.

[2] O. Vingsbo and S. Söderberg, “On fretting maps,” *Wear*, vol. 126, no. 2, pp. 131–147, 1988.

[3] O. Jin and S. Mall, “Effects of slip on fretting behavior: experiments and analyses,” *Wear*, vol. 256, no. 7–8, pp. 671–684, 2004.

[4] J. Madge, S. Leen, and P. Shipway, “A combined wear and crack nucleation–propagation methodology for fretting fatigue prediction,” *Int. J. Fatigue*, vol. 30, no. 9, pp. 1509–1528, 2008.

[5] J. Ding, W. S. Sum, R. Sabesan, S. B. Leen, I. R. McColl, and E. J. Williams, “Fretting fatigue predictions in a complex coupling,” *Int. J. Fatigue*, vol. 29, no. 7, pp. 1229–1244, 2007.

[6] P. M. Wavish, D. Houghton, J. Ding, S. B. Leen, E. J. Williams, and I. R. McColl, “A multiaxial fretting fatigue test for spline coupling contact,” *Fatigue Fract. Eng. Mater. Struct.*, vol. 32, no. 4, pp. 325–345, 2009.

[7] C. Ruiz, P. H. B. Boddington, and K. C. Chen, “An investigation of fatigue and fretting in a dovetail joint,” *Exp. Mech.*, vol. 24, no. 3, pp. 208–217, 1984.

[8] A. Cruzado, M. Hartelt, R. Wäsche, M. A. Urchegui, and X. Gómez, “Fretting wear of thin steel wires. Part 1: Influence of contact pressure,” *Wear*, vol. 268, no. 11–12, pp. 1409–1416, 2010.

[9] A. Cruzado, M. Hartelt, R. Wäsche, M. A. Urchegui, and X. Gómez, “Fretting wear of thin steel wires. Part 2: Influence of crossing angle,” *Wear*, vol. 273, no. 1, pp. 60–69, 2011.

[10] R. N. Burke and J. A. Witz, “Fretting fatigue of flexible pipe pressure armour,” in *Proceedings of the Third European Conference on Flexible Pipes, Unbilicals and Marine Cables - Materials Utilisation for cyclic and Thermal Loading*, 1995.

[11] S. M. O’Halloran, A. M. Harte, A. D. Connaire, and S. B. Leen, “Modelling of fretting in the pressure armour layer of flexible marine risers,” *Tribol. Int.*, 2016.

[12] M. O’Sullivan, “Meeting the future challenges of flexible pipe technology - advances in industry standards,” in *Proceedings of the Offshore Technology Conference (OTC)*, 2009.

[13] API, “Recomended Practices for Flexible Marine Risers, 17J,” *Am. Pet. Ind.*, 2009.

[14] H. Lange, S. Berge, T. Rogne, and T. Glomstaker, “Robust material selection in the offshore industry - flexible risers,” MARINTEK, SINTEF Materials and Chemistry, 2004.

[15] S. A. Lotveit and R. Bjaerum, “Second Generation Analysis Tool for Flexible Pipes,” in *Proceedings of the Second European Conference on Flexible Pipes, Umbilicals and Marine Cables-Structural Mechanics and Testing*, 1994.

[16] J. J. Féret and C. L. Bournazel, “Calculation of stresses and slip in structural layers of unbonded flexible pipes,” *J. Offshore Mech. Artic Eng.*, vol. 109, p. 263, 1987.

[17] S. D. R. Perera, U. P. Ferando, T. Sheldrake, and R. Clements, “An investigation into fretting behaviour in pressure armour wires of unbonded flexible pipes,” in *26th International Conference on Offshore Mechanics and Artic Engineering*, 2007.

[18] T. Zhang, P. E. McHugh, and S. B. Leen, “Computational study on the effect of contact geometry on fretting behaviour,” *Wear*, vol. 271, no. 9–10, pp. 1462–1480, 2011.

[19] I. R. McColl, J. Ding, and S. B. Leen, “Finite element simulation and experimental

validation of fretting wear," *Wear*, vol. 256, no. 11–12, pp. 1114–1127, 2004.
[20] K. N. Smith, P. Watson, and T. H. Topper, "Stress-strain function for fatigue of metals," *J. Mater.*, vol. 5, no. 4, p. 767–&, 1970.
[21] W. Sum, E. Williams, and S. Leen, "Finite element, critical-plane, fatigue life prediction of simple and complex contact configurations," *Int. J. Fatigue*, vol. 27, no. 4, pp. 403–416, 2005.
[22] J. Araújo, "The effect of rapidly varying contact stress fields on fretting fatigue," *Int. J. Fatigue*, vol. 24, no. 7, pp. 763–775, Jul. 2002.
[23] J. A. ARAUJO, D. NOWELL, and R. C. VIVACQUA, "The use of multiaxial fatigue models to predict fretting fatigue life of components subjected to different contact stress fields," *Fatigue Fract. Eng. Mater. Struct.*, vol. 27, no. 10, pp. 967–978, Oct. 2004.
[24] J. Araújo, "Analysis of pad size effects in fretting fatigue using short crack arrest methodologies," *Int. J. Fatigue*, vol. 21, no. 9, pp. 947–956, Oct. 1999.
[25] C. Paulin, S. Fouvry, and C. Meunier, "Finite element modelling of fretting wear surface evolution: Application to a Ti–6A1–4V contact," *Wear*, vol. 264, no. 1–2, pp. 26–36, Jan. 2008.
[26] C. Mary and S. Fouvry, "Numerical prediction of fretting contact durability using energy wear approach: Optimisation of finite-element model," *Wear*, vol. 263, no. 1–6, pp. 444–450, Sep. 2007.
[27] T. Zhang, N. M. Harrison, P. F. McDonnell, P. E. McHugh, and S. B. Leen, "Micro-macro wear-fatigue of modular hip implant taper-lock coupling," *J. Strain Anal. Eng. Des.*, vol. 49, no. 1, pp. 2–18, Oct. 2013.
[28] ASTM International, "ASTM E606-04 Standard Practice for Strain-Controlled Fatigue Testing," 2005. .
[29] S. S. Manson, "Fatigue: A complex subject—Some simple approximations," *Exp. Mech.*, vol. 5, no. 4, pp. 193–226, 1965.
[30] A. Cruzado, S. B. Leen, M. A. Urchegui, and X. Gómez, "Finite element simulation of fretting wear and fatigue in thin steel wires," *Int. J. Fatigue*, vol. 55, pp. 7–21, 2013.
[31] J. Ding, D. Houghton, E. J. Williams, and S. B. Leen, "Simple parameters to predict effect of surface damage on fretting fatigue," *Int. J. Fatigue*, vol. 33, no. 3, pp. 332–342, 2011.

Figures

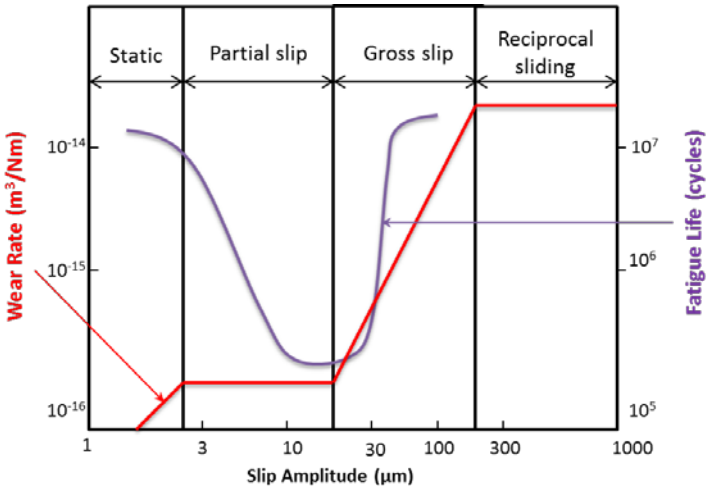

Figure 1. Schematic fretting map shows the effect of slip regime on fatigue life and wear rate [2].

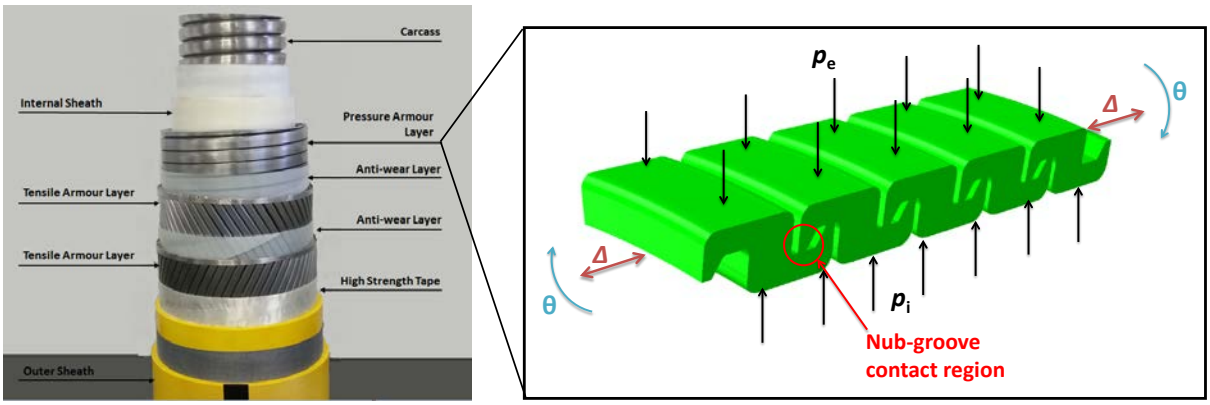

Figure 2. Photograph of a flexible marine riser cross section; loading conditions on pressure armour layer, where p_e - external pressure on risers, p_i - internal pressure on the riser, Δ - axial displacement of the pressure armour layer, θ - rotational displacement of the pressure armour layer.

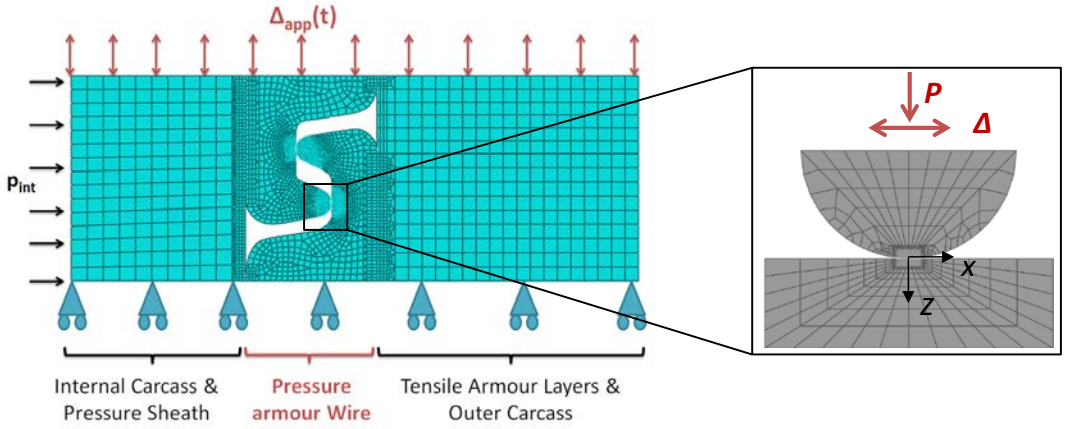

Figure 3. Axisymmetric local pressure armour model with a round on flat nub groove geometry.

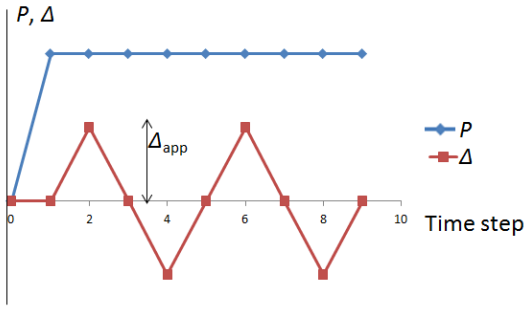

Figure 4. Applied stroke and loading history

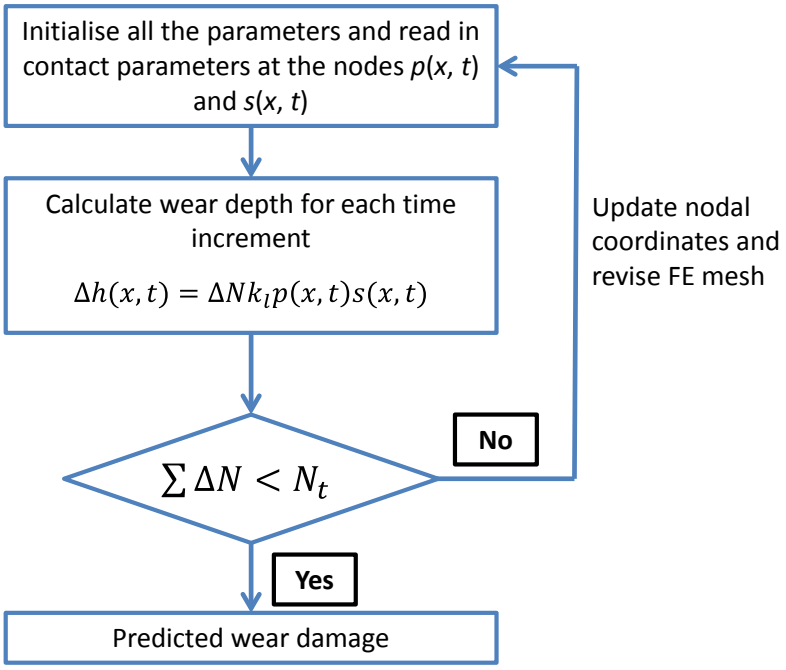

Figure 5. Methodology for implementation of the adaptive meshing technique to predict fretting wear damage.

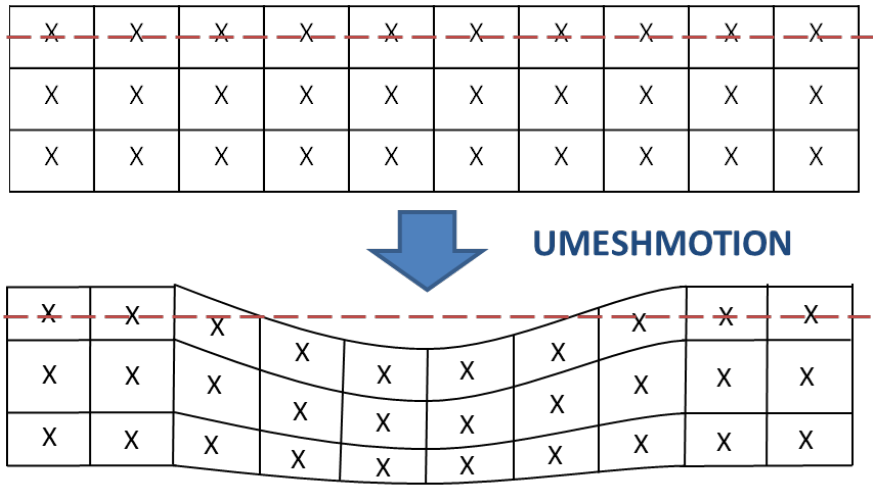

Figure 6. Finite element mesh as wear takes place for the adaptive meshing methodology [30].

(a) (b)

Figure 7. (a) Helically wound pressure armour wire in the dissected riser, and (b) pressure armour layer material extracted from the pipe

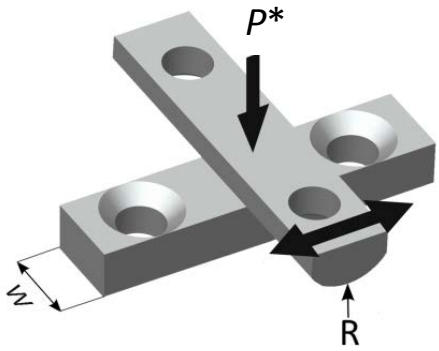

Figure 8. Cylinder on flat specimen configuration used for fretting wear tests.

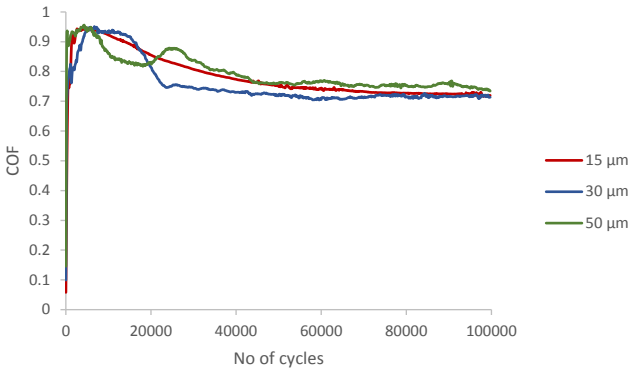

Figure 9. COF evolution with number of fretting cycles for a pressure armour layer representative material under normal load, P^* = 250 N and applied tangential displacements, Δ^* = 15, 30, 50 µm.

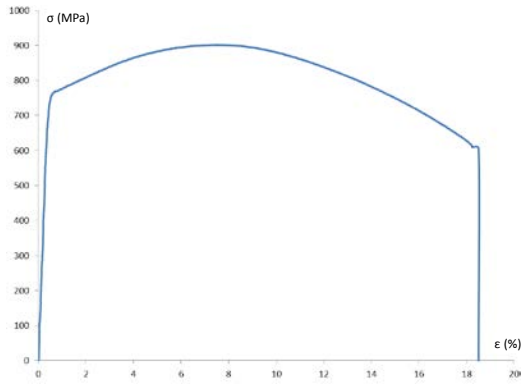

Figure 10. Monotonic tensile stress-strain curve for pressure armour material.

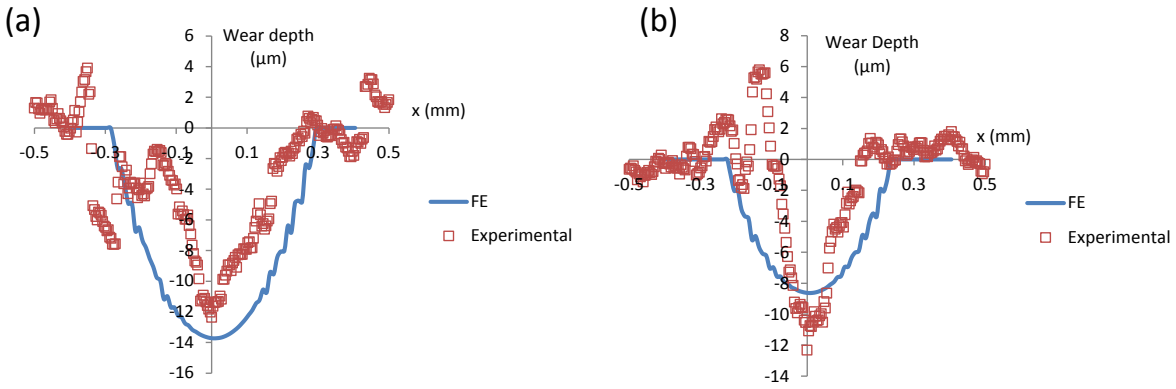

Figure 11. Comparison between finite element simulated wear scars and experimentally produced fretting wear scars for R = 6 mm after 10^5 cycles at 20 Hz and: (a) P^* = 500 N, Δ^* = 30 µm; and (b) P^* = 250 N, Δ^* = 15 µm.

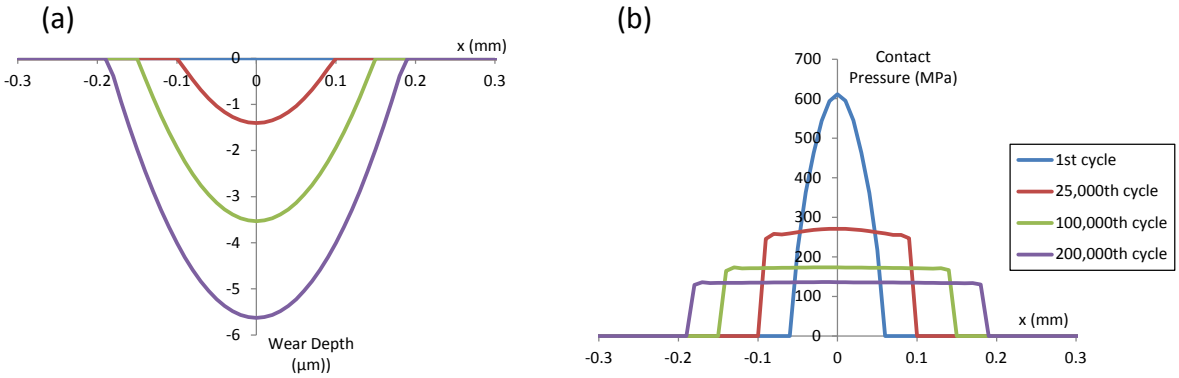

Figure 12. FE wear simulation results for gross slip (P = 50 N/mm and Δ = 10 µm) condition showing evolution of (a) wear scar; and (b) contact pressure.

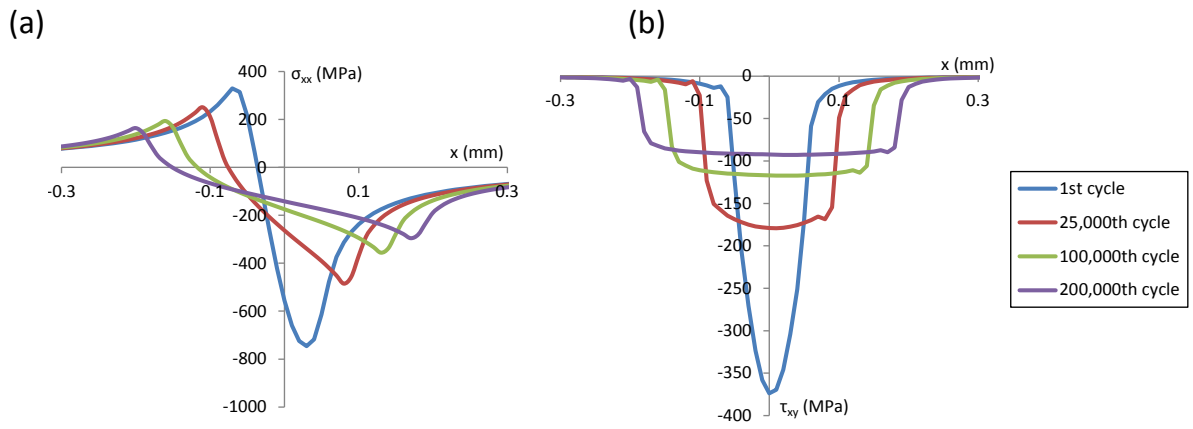

Figure 13. FE wear simulation results for gross slip (P = 50 N/mm and Δ = 10 μm) condition showing evolution of (a) tensile stress (σ_{xx}); and (b) shear stress (τ_{xy}).

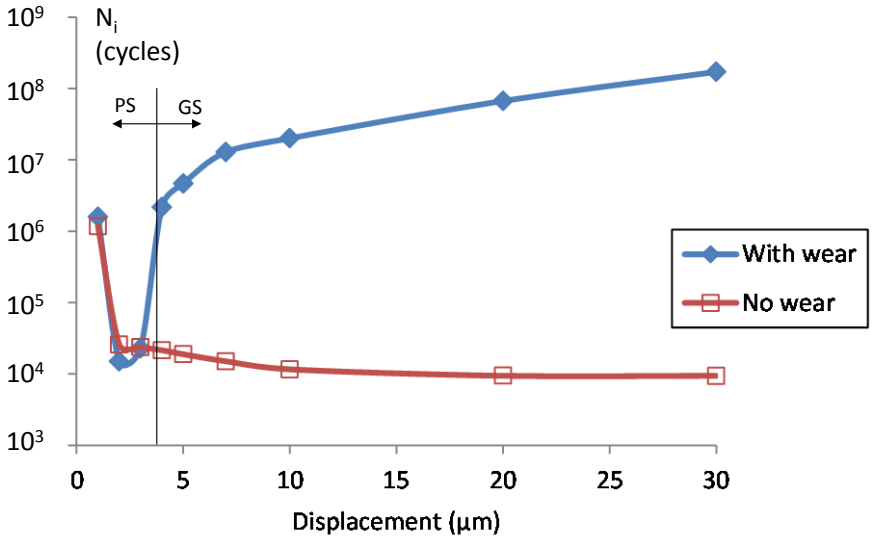

Figure 14. Predicted effect of applied tangential displacement on crack initiation life: (i) without effect of wear, and (ii) with effect of wear.

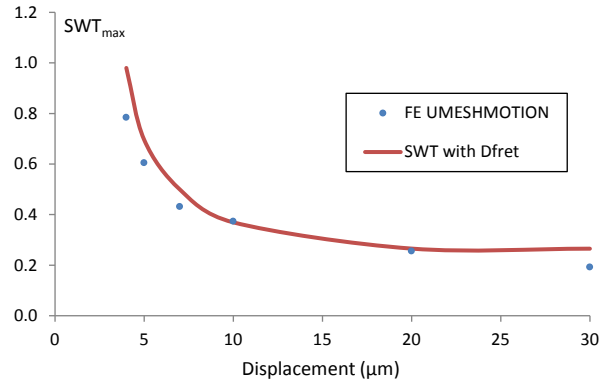

Figure 15. Comparison of effect of displacement on wear simulation SWT_{max} and maximum SWT-D_{fret} value.

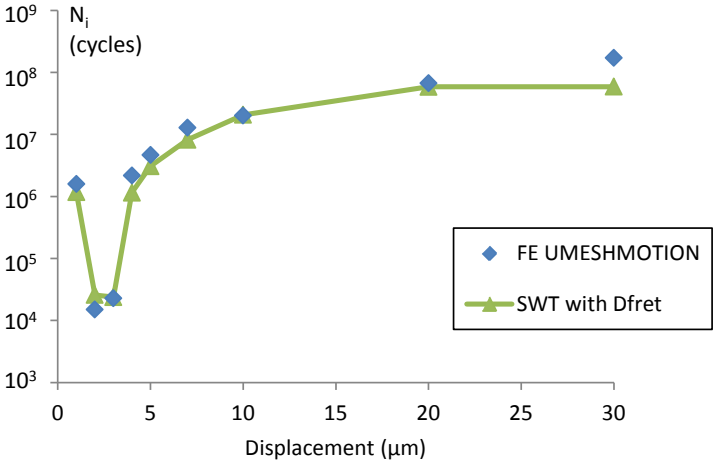

Figure 16. Comparison of effect of displacement on fretting crack initiation life calculated using wear simulated SWT and modified SWT-D_{fret} parameter.

Tables

Table 1. Chemical composition of pressure armour material and EN8.

Material	Element	C	Mg	Si	P	S
Pressure armour	Weight (%)	0.409	0.761	0.304	0.0137	0.0071
EN8		0.36-0.44	0.60-1.00	0.10-0.40	0.050 Max	0.050 Max

Table 2. Geometry and loading conditions on cylinder-on-flat on fretting test.

P^* (N)	Δ^* (μm)
250	15, 30, 50
500	15, 30, 50

Table 3. Identified low- and high-cycle fatigue constants for pressure amour wire.

Parameter	Value
σ'_f	1710 MPa
ε'_f	0.2355
b	-0.12
c	-0.5742

Table 4. D_{fret} constants for pressure armour wire.

Parameter	Value
$(\tau\delta)_{th}$	0.4 MPa mm
C	0.05 MPa^{-1} mm^{-1}
m	-0.85